Numerical studies of the two-dimensional XY model with symmetry-breaking fields

T. Ala-Nissila
Research Institute for Theoretical Physics, University of Helsinki, P.O. Box 9 (Siltavuorenpenger 20 C), FIN-00014 University of Helsinki, Finland;
Department of Physics, Brown University, Box 1843, Providence, Rhode Island 02912;
and Department of Electrical Engineering, Tampere University of Technology, P.O. Box 692, FIN-33101 Tampere, Finland

E. Granato
Laboratório Associado de Sensores e Materiais, Instituto Nacional de Pesquisas Espaciais, 12225 - São José dos Campos, São Paulo, Brazil

K. Kankaala
Center for Scientific Computing, P.O. Box 405, FIN-02101 Espoo, Finland
and Department of Electrical Engineering, Tampere University of Technology, P.O. Box 692, FIN-33101 Tampere, Finland

J. M. Kosterlitz and S.-C. Ying
Department of Physics, Brown University, Box 1843, Providence, Rhode Island 02912
(Received 26 April 1994)

We present results of numerical studies of the two-dimensional XY model with four- and eightfold symmetry-breaking fields. This model has recently been shown to describe hydrogen-induced reconstruction on the W(100) surface. Based on mean-field and renormalization-group arguments, we first show how the interplay between the anisotropy fields can give rise to different phase transitions in the model. When the fields are compatible with each other there is a continuous phase transition when the fourth-order field is varied from negative to positive values. This transition becomes discontinuous at low temperatures. These two regimes are separated by a multicritical point. In the case of competing four- and eightfold fields, the first-order transition at low temperatures opens up into two Ising transitions. We then use numerical methods to accurately locate the position of the multicritical point, and to verify the nature of the transitions. The different techniques used include Monte Carlo histogram methods combined with finite-size scaling analysis, the real-space Monte Carlo renormalization-group method, and the Monte Carlo transfer-matrix method. Our numerical results are in good agreement with the theoretical arguments.

I. INTRODUCTION

In two dimensions, conventional long-range order cannot exist in continuous spin models $[O(n),\ n \geq 2]$ because it is destroyed by spin wave excitations.[1–3] However, Kosterlitz and Thouless[1] proposed that in the XY $[O(2)]$ model there is a phase below the critical temperature where topological long-range order can be defined. The vanishing of this order occurs via the Kosterlitz-Thouless (KT) transition. Physical systems where the KT transition occurs are numerous; they include superfluid ^{4}He films, Josephson junction arrays, superconducting transitions of type II, and various phase transitions on surfaces and adsorption layers.

In many cases, the realization of the XY model is accompanied by various symmetry-breaking fields, whose effect is very complicated as demonstrated qualitatively by Josè *et al.*[4] For example, it was recognized already at an early stage[4] that the presence of a fourfold field restores a conventional phase transition, but with continuously varying critical exponents. In contrast, a sixfold symmetry-breaking field opens up the KT transition into two parts: at high temperatures, the transition remains XY type, but at low enough temperatures it is into a discrete planar phase in which the system orders along one of the six preferred directions.[5] Both of these situations have been realized in experimental systems; fourfold fields are known to be present in surface structural phase transitions whereas liquid crystals provide a case where the sixfold field exists.

The effects of symmetry-breaking fields are further complicated by the existence of *higher order* multiples of the fields, which are allowed by symmetry. In most cases, since these fields are irrelevant if lower order fields are present, their influence has been neglected. However, if it happens that the lowest order symmetry-breaking field vanishes, the higher harmonics can become relevant at low enough temperatures.[4] A demonstration of this fact is the study of Selinger and Nelson[5] who modeled a phase transition occurring in liquid crystals by an XY model with six- and twelvefold symmetry-breaking fields. They found a rich behavior of the phase diagram depending on whether or not the two fields are compatible with each other.

We have recently developed[6] a lattice Hamiltonian for the adsorption system H/W(100), which is based on the

XY model with a fourfold symmetry-breaking field, and its higher harmonics. We have argued that the essential physics of this model is dictated by an interplay between the fourfold and the eightfold fields, in a manner very similar to that of Ref. 5. The intriguing aspect of this model is that the strengths of the symmetry fields — the fourfold field in particular — are *tunable* by changing the amount of adsorbed hydrogen. In fact, it was demonstrated that the fourth-order field *vanishes* at a hydrogen coverage of about 0.1 ML for this system. This system thus provides an ideal example for studying the effect of interplay between symmetry-breaking fields within the XY model.

The purpose of the present work is to conduct a detailed, quantitative study of the two-dimensional XY model with four- and eightfold anisotropy fields. We shall first discuss in detail how the interplay between these two anisotropy fields dictates the nature of the phase diagram at low temperatures where the eightfold field is relevant in the renormalization-group sense. We give both mean-field and renormalization-group arguments in explaining how it is possible to obtain either a discontinuous or two continuous Ising transitions at low temperatures due to the interplay between the anisotropy fields. Namely, when the four- and eightfold fields are compatible with each other and do not compete, this gives rise to a first-order transition at $h_4 = 0$ as we pass from negative (positive) values of the fourfold field to positive (negative) with a finite h_8 field. However, when the two fields are competing with each other, the first-order transition opens up into two Ising transitions with an intermediate phase in between.

Following analytic arguments, we proceed to simulate the XY model with symmetry-breaking fields using the Monte Carlo method with the Wolff updating algorithm which is generalized to include contributions from the anisotropy fields. We employ finite-size scaling arguments to locate the multicritical point in this model. These results are further corroborated by Monte Carlo transfer-matrix (MCTM) studies. We also verify the existence of the continuous Ising transition in the case of competing anisotropy fields by using both the MCTM and real-space Monte Carlo renormalization-group methods. Our results are in good agreement with theoretical predictions, and also consistent with available experimental data for the H/W(100) adsorption system.

II. MODEL HAMILTONIAN AND QUALITATIVE RENORMALIZATION-GROUP ANALYSIS

The Hamiltonian of the XY model with four- and eightfold anisotropy fields can be written as

$$H = -K\sum_{\langle i,j\rangle}\cos(\phi_i-\phi_j) - h_4\sum_i\cos(4\phi_i) + h_8\sum_i\cos(8\phi_i), \tag{1}$$

where K is the XY coupling constant between nearest neighbors, ϕ_i are the angle variables defined by the individual spin vectors $\vec{\sigma}_i = (\cos\phi_i, \sin\phi_i)$ on site i, h_4 and h_8 are the four- and eightfold symmetry-breaking fields, respectively, and we have subsumed the temperature into the coupling constants and fields. The summation $\langle i,j\rangle$ goes over the nearest neighbors, and the summations i are over all lattice sites.

We will first discuss mean-field theory to obtain a qualitative picture of the critical phenomena that Eq. (1) gives rise to. Our purpose is to give insight into the underlying physics which is dictated by the interplay between the anisotropy fields. These arguments correspond to the case where both fields are always assumed to be relevant, and will thus give correct qualitative behavior at low temperatures only. There are two possible scenarios depending on the anisotropy potential $V(\phi)$ of Eq. (1), defined by

$$V(\phi) \equiv -h_4\cos(4\phi) + h_8\cos(8\phi). \tag{2}$$

Namely, when h_4 is negative it favors spins aligning along the directions $\phi = \pi/4 + n\pi/2$, $n = 0, 1, ...$, whereas a positive h_4 favors $\phi = n\pi/2$, $n = 0, 1, ...$ The eightfold field has two possibilities as well. When $h_8 < 0$ the favored orientations are $\phi = n\pi/4$, $n = 0, 1, ...$, which are exactly the directions favored by either a negative or a positive fourfold field. We say that in this case the anisotropy fields are *noncompeting* or *compatible* with each other. For $h_8 > 0$ the favored orientations are $\phi = \pi/8 + n\pi/4$, $n = 0, 1, ...$ As these are different from those favored by the fourfold field, *competition* will set in when the four- and eightfold fields are of the same order of magnitude.

We first consider the case of a negative, i.e., noncompeting, h_8. In Fig. 1(a), we show the anisotropy potential $V(\phi)$ as a function of the angle ϕ for various values of h_4, given a fixed h_8. The local minima at $\phi = 0$ and at $\phi = \pm\pi/4$ are clearly visible. When $h_4 > 0$, the minima at $\phi = 0$ are deeper, whereas for $h_4 < 0$ the minima at $\phi = \pi/4$ are deeper. As h_4 passes through zero from $h_4 > 0$ to $h_4 < 0$, there is a first-order transition from one minimum to another.

In the case of a positive or competing eightfold field, the situation is more complicated. The behavior of the potential $V(\phi)$ for fixed $h_8 > 0$ and various values of h_4 is shown in Fig. 1(b). For $h_4 > 4|h_8|$, there is only one minimum at $\phi = 0$, and one at $\phi = \pm\pi/4$ for $h_4 < -4|h_8|$. But now as the fourfold field passes through $h_4 = 4|h_8|$, the single minimum splits into two at $\phi = \pm\phi_0'$. By minimizing the anisotropy potential $V(\phi)$, we can show that these new minima begin to form at

$$\phi = \pm\tfrac{1}{4}\left|\cos^{-1}\left(\frac{h_4}{4h_8}\right)\right| \equiv \pm\phi_0'. \tag{3}$$

At the other boundary where h_4 passes through $-4|h_8|$, the same argument applies except that ϕ_0' now measures the deviation from $\pi/4$. The first-order transition for the compatible field case [cf. Fig. 2(a)] has now opened up into two continuous transitions with an intermediate phase in between [cf. Fig. 2(b)].

We will next show explicitly that the continuous phase

transition belongs to the universality class of the two-dimensional Ising model. We can approach the transition boundaries either from the phase where $h_4 > 0$ where the preferred orientation of spins is along $\phi = 0, \pi/2, \ldots$, or from the phase where $h_4 < 0$ and the favored directions are then $\phi = \pi/4, 3\pi/2, \ldots$. Let us consider the former possibility. For large h_4, the system is in the energy minimum at $\phi = 0$. When we approach the transition ($h_4 \to 0$), two minima form at $\phi = \pm\phi_0'$. Let us consider the contribution to the partition function due to these new minima. The Boltzmann weights can be written as $\exp\{K\cos[(s_i - s_j)\phi_0']\}$ where $s_i = \pm 1$. We denote these weights by $W[s]$ where $s = s_i - s_j = 0, 2$. For two neighboring spins at the same minimum,

$$W[0] = \exp(K), \tag{4}$$

while for two opposite spins

$$W[2] = \exp(K\cos 2\phi_0'). \tag{5}$$

The equivalent Ising coupling constant is thus $J = K\sin^2\phi_0'$. Since the argument is valid in the limit $K \to \infty$ only, we will later numerically verify the nature of the Ising transition predicted here.

Next, we present more quantitative renormalization-group (RG) arguments which are a direct extension of the work by Selinger and Nelson.[5] At high temperatures (where K is small), only the fourfold field is relevant in the RG sense, and the long-range order in the system is dictated by h_4 alone. At some temperature corresponding to K_m the eightfold field becomes relevant. For lower temperatures (larger values of K) and for finite h_4 and h_8, the nature of the phase diagram is determined by the interplay between these two fields as qualitatively discussed above. Any anisotropy field h_p of order p will obey the RG recursion relation[4]

$$h_p' = b^{\lambda_p} h_p, \tag{6}$$

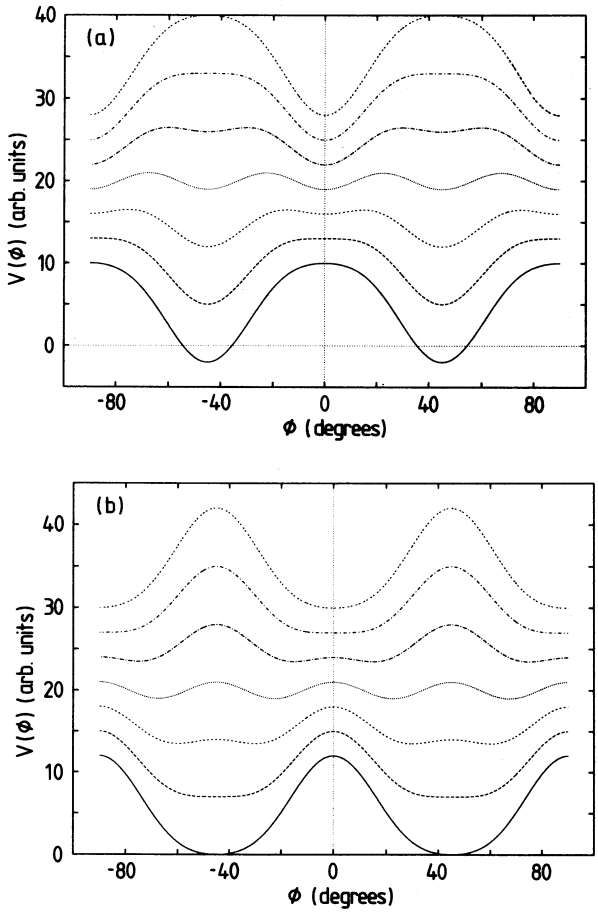

FIG. 1. (a) A schematic figure of the anisotropy potential $V(\phi)$ of Eq. (2), for the case of noncompeting fields with $h_8 = -1$. The curves from bottom to the top are for $h_4 = -6$, -4, -2, 0, 2, 4, and 6, respectively. The transition at $h_4 = 0$ is abrupt. (b) The anisotropy potential for competing fields with $h_8 = +1$. The curves are for the same values of h_4 as in (a). The transition around $h_4 = 0$ is continuous.

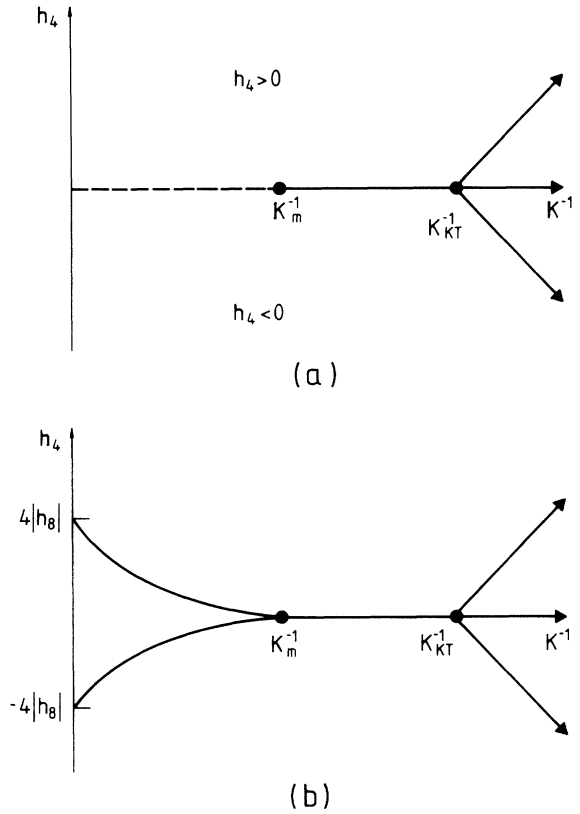

FIG. 2. (a) A schematic phase diagram for the Hamiltonian Eq. (1) on the h_4-K^{-1} plane, with a fixed noncompeting $h_8 < 0$. For finite values of h_4, the two transition lines beyond the Kosterlitz-Thouless transition point $K_{KT}^{-1} < \pi/2$ belong to the universality class of the XY model with a fourfold symmetry-breaking field. Between K_{KT}^{-1} and the multicritical point K_m^{-1}, there is a line of pure XY transitions. Below K_m^{-1}, the eightfold field is relevant and there is a line of first-order transitions. The lower bound for K_m^{-1} is $\pi/8$ [cf. Eq. (9)]. (b) The counterpart of the phase diagram of (a) for the case of a fixed, competing $h_8 > 0$. Below K_m^{-1}, where h_8 is relevant, the first-order transitions open up into two lines of continuous Ising transitions, which terminate at $\pm 4|h_8|$.

where h_p' is the field obtained after a RG iteration, b is a constant, and

$$\lambda_p = 2 - \frac{1}{4\pi K}p^2. \tag{7}$$

When the parameter $\lambda_p > 0$, the field h_p' will increase as iterations proceed, and the pth anisotropy field is a *relevant* variable.[4] However, as the temperature increases, higher order fields become *irrelevant* ($\lambda_p < 0$), and the respective h_p' will decrease with iteration. On the other hand, it can easily be seen that at $K = \infty$ all symmetry-breaking perturbations are relevant. If $\lambda_p = 2 - p^2/(4\pi K) = 0$, we get the temperature $K_{m,p}^{-1}$ below which the field h_p is relevant, i.e., it is *marginally* relevant at that point:[4]

$$K_{m,p}^{-1} = \frac{8\pi}{p^2}. \tag{8}$$

We can conclude that the four- and eightfold anisotropy fields are relevant at all temperatures $K^{-1} < K_{m,4}^{-1} = \pi/2$ and $K^{-1} < K_{m,8}^{-1} = \pi/8$, respectively. The results for the XY model with only the fourfold field h_4 are well known.[4] The continuous phase transition into an ordered state ($h_4 \neq 0$) along the critical lines terminating at $K_{\mathrm{KT}}^{-1} < K_{m,4}^{-1} = \pi/2$ belongs to the universality class of the XY model with a cubic anisotropy field, where K_{KT}^{-1} is the (true) order-disorder transition temperature for the pure XY model. Along the critical line $h_4 = 0$ we have a series of continuous XY transitions for all $K^{-1} < K_{\mathrm{KT}}^{-1}$ (cf. Fig. 2). In the other limit where $h_4 \to \infty$, the model becomes a four-state clock model which can be shown to decouple into two Ising models.[7]

With the inclusion of the eightfold field, different scenarios occur depending on the signs of h_4 and h_8. For the remainder of this paper, we will denote by K_m^{-1} the true value of the coupling constant where the eightfold field becomes relevant. For $K^{-1} < K_m^{-1}$, both h_4 and h_8 are relevant. If h_8 is positive, the renormalized potential $V^*(\phi)$ is similar to that of Fig. 1(b) with two continuous Ising transitions. In the limit $K \to \infty$, we obtain the exact mean-field result: the transition occurs at $h_4 = \pm 4|h_8|$. In the other limit $K \to K_m$, it can be shown[5] that to lowest order in $|h_8|$ we have

$$K_m^{-1} = \frac{\pi}{8} + B|h_8|, \tag{9}$$

where $B > 0$ is a constant which can be estimated to be $O(1)$. The upper bound for K_m^{-1} is the Kosterlitz-Thouless transition temperature $K_{\mathrm{KT}}^{-1} < \pi/2$ for this model. The lower bound, on the other hand, is given by the zero-field estimate $K_m^{-1}(h_8 = 0) = \pi/8$. The corresponding phase diagram is shown schematically in Fig. 2(b).

For a negative h_8 and for $K^{-1} < K_m^{-1}$, the system fluctuates in the minima of Fig. 1(a). The location of the deepest minimum changes as h_4 passes through $h_4 = 0$, and we expect a first-order phase transition. Selinger and Nelson[5] have in fact shown that in this case there is a discontinuity in the order parameter across the transition. This discontinuity vanishes exponentially as $K \to K_m$,[5] thus making it very difficult to numerically locate K_m. The phase diagram corresponding to this noncompeting case is depicted in Fig. 2(a).

In the remainder of this paper, we will perform detailed numerical studies of two particular aspects of the phase diagrams shown in Figs. 2(a) and 2(b). The first concerns the exact location of the multicritical point K_m for $h_4 = 0$, for a finite h_8. The second is the verification of the Ising-like nature of the low temperature transition lines in Fig. 2(b) for the competing case.

III. LOCATION OF THE MULTICRITICAL POINT

To quantitatively locate the multicritical point K_m, we have performed extensive Monte Carlo simulations of Eq. (1), by adopting a modified Wolff algorithm. The Wolff algorithm was originally developed for isotropic, continuous spin systems such as the XY model.[8] In our case, we have added symmetry-breaking fields to the model. This is accounted for by modifying the Wolff cluster update algorithm in the following way. We divide the Hamiltonian of Eq. (1) into two parts, the isotropic part H_{XY},

$$H_{XY} = -K\sum_{\langle i,j\rangle}\cos(\phi_i - \phi_j), \tag{10}$$

and the anisotropic part $H_{4,8}$,

$$H_{4,8} = -h_4\sum_i \cos(4\phi_i) + h_8\sum_i \cos(8\phi_i). \tag{11}$$

We form the Wolff cluster for the isotropic part H_{XY} in the usual fashion using a cluster labeling technique similar to the "ants in the labyrinth" scheme.[9] We then calculate the change in the energy due to the anisotropy fields for the old and the proposed new cluster as

$$\Delta H_{4,8} = H_{4,8}^{\mathrm{new}} - H_{4,8}^{\mathrm{old}}. \tag{12}$$

Whether or not the cluster is flipped is determined by applying the standard Metropolis acceptance criterion to this energy difference. It is easy to verify that this combined algorithm satisfies detailed balance and is ergodic.

It has recently been shown[10] that the Wolff algorithm performs poorly for anisotropic XY models at low temperatures. It probes the phase space effectively but, in the presence of strong anisotropy fields, reaching thermal equilibrium from an initial state can take very long. The Metropolis algorithm, on the other hand, reaches local equilibrium rapidly but fails to search the phase space extensively. We have overcome these problems by a scheme where Wolff and Metropolis algorithms are simply combined by inserting several Metropolis local update sweeps after a certain amount of Wolff steps. A similar approach has also been suggested previously in Ref. 11.

To locate the multicritical point of the XY model with anisotropy fields, we use the method of Lee and Kosterlitz.[12] In this scheme, the "free energy" F for a given system of linear size L with order parameter Ψ and with periodic boundary conditions can be expressed as

$$\exp[-F(\Psi,L,N)] = NZ^{-1}(\beta)\sum_E \Omega(E,\Psi)\exp(-\beta E), \tag{13}$$

where N is the number of samples (configurations), $Z(\beta)$ is the partition function, $\Omega(E,\Psi)$ is the number of states with energy E, and we assume that the transition is driven by an external field. In the following, we shall for simplicity drop the N dependence of F. F differs from the actual bulk free energy but its *shape* is identical to that of the bulk free energy and thus is also the *difference* ΔF [see Eq. (15) below]. The "free energy" has two minima due to the two coexisting phases. These minima, located at Ψ_1 and Ψ_2, are separated by a maximum at Ψ_m. In the thermodynamic limit the double minima structure vanishes at the transition points but in a finite system it may persist even above the transition temperature. In this method it is precisely this property that is exploited to reveal the order of the transition for a finite system. More specifically, the free energy can be expanded below the transition where the correlation length $\xi \ll L$ as

$$F(\Psi,L) = L^d f_0(\Psi,g) + L^{d-1} f_1(\Psi,g) + \cdots, \tag{14}$$

where $f_0(\Psi,g)$ is the bulk free energy density, $f_1(\Psi,g)$ is a surface term which has a maximum at $\Psi_1 < \Psi_m < \Psi_2$, and g is a scaling field $g \propto (T-T_C)$. It can then be shown that the free energy has a minimum on both sides of the maximum Ψ_m, and that the height difference between the minima and the maximum is

$$\begin{aligned}\Delta F(L) &\equiv F(\Psi_m,L) - F(\Psi_1,L) \\ &= A(g)L^{d-1} + B(g)L^{d-2} + \cdots .\end{aligned} \tag{15}$$

This expansion holds for first-order transitions when $\xi \ll L$, and the free energy difference $\Delta F(L)$ is an increasing function of the system size L. Even for $L \ll \xi$, $\Delta F(L)$ is an increasing function of L. Thus, at the first-order transition point when $F(\Psi_1,L) = F(\Psi_2,L)$, $\Delta F(L)$ is an increasing function of L. In the disordered phase, the free energy difference $\Delta F(L)$ *decreases* as a function of L.

Near a fixed point describing a continuous transition, a scaling form can be developed for the singular part of the free energy.[12] Its analytic expansion gives $\Delta F(L) = a - bgL^{1/\nu} + O(g^2L^{2/\nu})$, where a and b are L-independent constants. This form is appropriate for $L \ll \xi$, where $g > 0$ for $K < K_m$ and $g < 0$ for $K > K_m$. Thus, we expect that $\Delta F(L)$ increases with L in the low temperature phase. However, for our model the behavior in the vicinity of K_m is expected to be very complicated, and a finite-size scaling form has not been developed. Naively, we would expect that because $1/\nu = 0$ and $\ln(\xi) \sim g^{-1/2}$, the barrier $\Delta F(L)$ will increase as $g\ln^2(L)$. For $K > K_m$, however, $\Delta F(L)$ must increase more rapidly with L eventually crossing over to the linear behavior of Eq. (15) for $L \gg \xi$ deep into the first-order regime. We will use this property of $\Delta F(L)$ and change K at $h_4 = 0$ to locate K_m, as explained below.

To facilitate the use of the finite-size scaling technique of Lee and Kosterlitz, we calculated the histogram of the order parameter $\Phi = (1/L^2)\sum_i \cos 4\phi_i$ summed over the lattice by dividing the interval $[0,1]$ into 200 equal bins, and putting each value into its respective bin. Thus we can construct a histogram which shows the double peak structure. This histogram is essentially an approximation of the partition function. By taking the negative of the logarithm of this histogram, we obtain an approximation for the free energy distribution $F(\Psi,L)$ of the system [cf. Eq. (13)]. As we reside on the transition line at $h_4 = 0$, the two peaks of $F(\Psi,L)$ are equally high, and we can readily calculate the difference $\Delta F(L)$ given in Eq. (15). For the eightfold field, we used the value $h_8 = -0.15$. When using the combined algorithm, we first did 3000 Metropolis steps to reach a local equilibrium and then continued with 5000 Wolff cluster formations with 10 Metropolis steps after each 1000 cluster formations. All this information was discarded. The data were averaged over 1 000 000 cluster formations so that after every 1000 Wolff cluster formations ten Metropolis steps followed. We calculated the order parameter histogram for several systems of sizes $L = 8$, 12, 16, 24, 32, 48, and 64 at various temperatures along the line $h_4 = 0$. From these data we can then deduce $\Delta F(L)$. In the first-order regime and in two dimensions, it should scale linearly with increasing L. If the transition is continuous, the double peak structure should vanish in the limit $L \to \infty$. We also studied the distribution of angles by constructing a histogram of each individual angle ϕ_i.

Our main results are depicted in Figs. 3(a)–3(c). Typical histograms for various system sizes are shown in Figs. 3(a) and 3(b), and the extracted energy barriers $\Delta F(L)$ as a function of the linear system size L in Fig. 3(c), for the present case of noncompeting anisotropy fields. All the $\Delta F(L)$'s were calculated by fitting an eight-order polynomial to the data. All data points are averages of about 10^6 configurations. The energy difference increases with L for temperatures corresponding to $K \geq 2.3$, which indicates a first-order regime. The behavior of $\Delta F(L)$ at temperatures corresponding to $K \leq 2.2$ indicates, on the other hand, a regime where the transition is continuous. At $K = 2.2$, $\Delta F(L)$ first seems to increase with L up to $L = 12$ and then decrease for larger L, although within error bars it is almost constant. At $K = 2.1$, no double peak structure exists. We also analyzed the size dependence of the multicritical point K_m. By fitting $\Delta F(L)$ vs the logarithm of inverse temperature K for $L = 8, 12, 16, 24, 48, 64$, we were able to determine the multicritical point $K_m(L)$ for each system size. From this we estimated the multicritical point by scaling these data against $1/L$. We conclude that

$$K_m = 2.1 \pm 0.1, \tag{16}$$

which is the main result of this section. It is also well within the theoretical bounds $2/\pi < K_m < 8/\pi$, as expected.

Finally, we should note that the accuracy of the result suffers from severe fluctuations in the vicinity of the multicritical point, in particular for the largest systems. This inhibits the use of histogram techniques for extrapolation.[13]

IV. ISING TRANSITION IN THE CASE OF COMPETING ANISOTROPY FIELDS

The other scenario for our model is the case where the anisotropy fields are competing. It was shown analytically that the first-order transition at low temperatures opens up to two Ising transitions with an intermediate phase in between. In this intermediate phase the long-range order is dictated by the eightfold field. To see this transition numerically, we chose a finite fourfold field $h_4 = 0.06$ which favors the orientations $\phi_i = 0, \pi/2$, etc., for the individual spins. The competing eightfold field is chosen to be equal in magnitude to the one used in the noncompeting case, i.e., $h_8 = 0.15$. We try to locate the corresponding Ising transition temperature K_I^{-1} by scanning the inverse temperature K. K_I should be well above our estimate of $K_m \approx 2.1$ [cf. Fig. 2(b)]. For this calculation, we used the Monte Carlo renormalization-group (MCRG) scheme proposed by Binder.[14] Consider the XY spins $\vec{\sigma}_i = (\cos\phi_i, \sin\phi_i)$ on a two-dimensional lattice which is divided into subcells or blocks of (linear) size L_B. Let us first define a block variable

$$\Phi_{L_B} = \frac{1}{L_B^2} \sum_{i \in L_B} \psi_i, \tag{17}$$

where ψ_i is a measure for the local order in the system. We can then define an order parameter for each block size as $\Psi_{L_B} = \langle \Phi_{L_B} \rangle$, where angular brackets again denote a configurational average. We studied different moments of the block variables Φ_{L_B}, and constructed the fourth- and sixth-order cumulants U_{L_B} and V_{L_B} for each block size

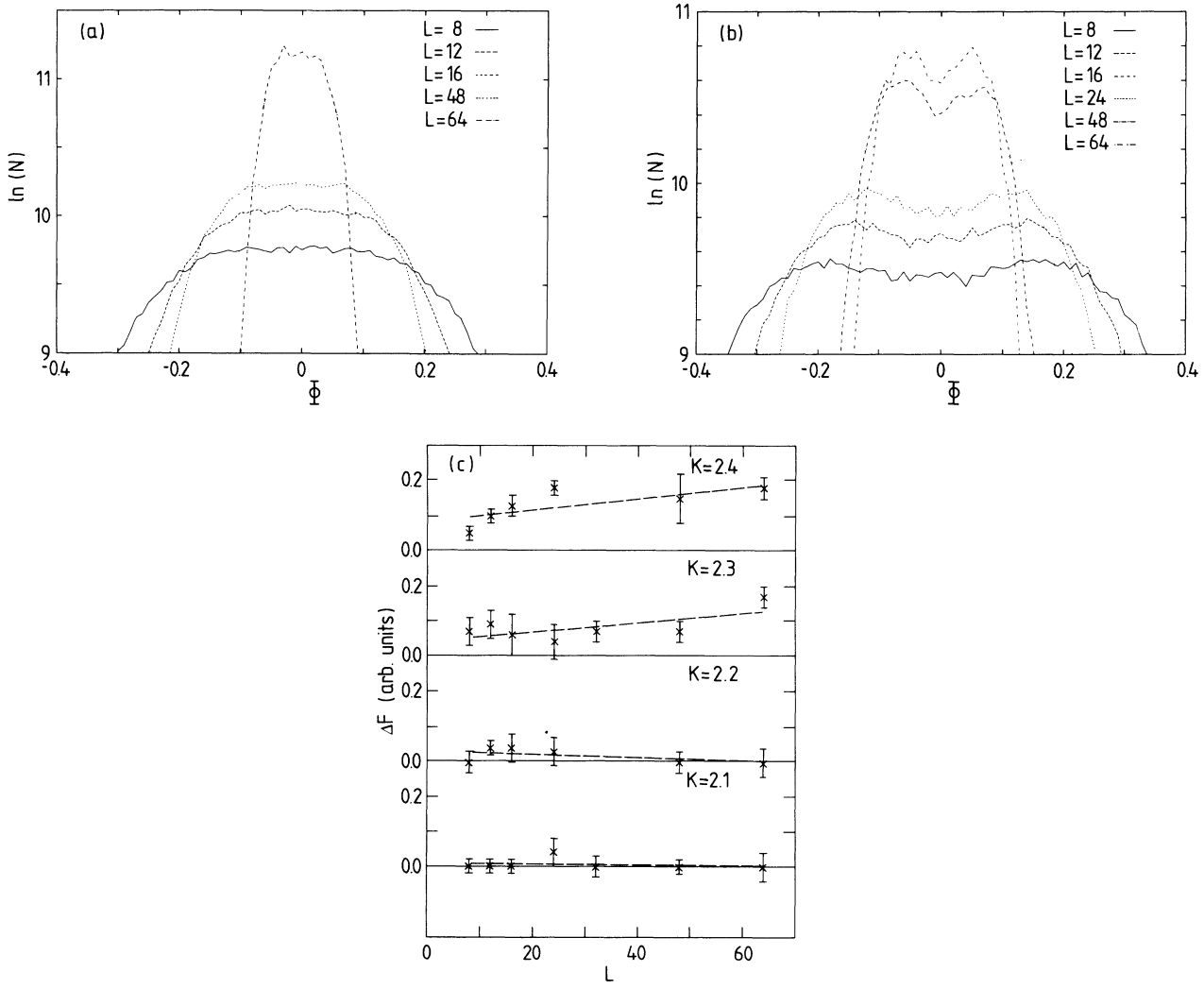

FIG. 3. (a) Logarithm of the histogram of the local order parameter $\Phi = (1/L^2)\sum_i \cos 4\phi_i$ [cf. Eq. (13)], at $K = 2.1$ for system sizes $L = 8, 12, 16, 48, 64$, with $h_4 = 0.06$ and $h_8 = -0.15$. N is the number of samples in each bin. (b) Logarithm of the histogram of the local order parameter $\Phi = (1/L^2)\sum_i \cos 4\phi_i$ at $K = 2.4$ for system sizes $L = 8, 12, 16, 24, 48, 64$, with $h_4 = 0.06$ and $h_8 = -0.15$. (c) The free energy barriers $\Delta F(L)$ [cf. Eq. (15)] extracted from polynomial fits to the histograms of the order parameter, plotted against L. Here $h_4 = 0$ and $h_8 = -0.15$, corresponding to (a). Above $K_m \approx 2.2$, the barriers clearly start increasing, indicating the onset of a first-order transition. See text for details.

as in Ref. 14. The variation of these two cumulants as a function of the block size L_B gives a flow diagram analogous to that of a renormalization-group method. These cumulants approach zero above T_C as the block size increases. Below T_C, both cumulants tend to nonzero values, $U_{L_B} \to 2/3$ and $V_{L_B} \to 8/15$ as $L_B \to \infty$. At the critical point T_C, the cumulants approach nontrivial fixed point values U^* and V^*. Thus, the behavior of the cumulants is reminiscent of the renormalization-group flows under subsequent transformations of the length scale. One can also estimate the correlation length exponent ν from the data in the vicinity of U^* by noting that[14]

$$\frac{U_{L'_B} - U^*}{U_{L_B} - U^*} \simeq b^{(1-\alpha)/\nu}, \tag{18}$$

for subsystem blocks of size $L'_B = L_B/b$, and by using the scaling relation $\alpha = 2 - \nu d$.

For the block variable we chose

$$\Phi_{L_B} = \frac{1}{L_B^2} \sum_i (\sin \phi_i) . \tag{19}$$

This order parameter, when the angles are folded between $-\pi/4 < \phi < \pi/4$, is zero in the high temperature phase and finite in the low temperature phase when a single domain dominates below and above the transition. We studied the fourth- and sixth-order cumulants U_{L_B} and V_{L_B}. From the flows of these cumulants as a function of the inverse linear size of the block, we can deduce the nontrivial fixed point value from which we can further extract K_I.

At low temperatures, the simulations suffer from high barriers between different regions of the phase space, which we tried to overcome by using the combined algorithm. We first used 5000 Metropolis steps to bring the configuration to a local equilibrium, and then continued with 3000 Wolff cluster formations before we started to collect data. The data were averaged over 100 000 cluster formations, and after every 1000 cluster moves ten thermalizing Metropolis steps were completed.

The flow of the fourth-order cumulants is depicted in Fig. 4. We can readily see that the value of K at which the transition takes place is $K_I \in [4.9, 5.0]$. A more detailed extraction of K_I was done by studying the ratio $U_{L'_B}/U_{L_B}$ where $L'_B \in [L_B, 64]$ and $L_B = 2, 4, 6, 8, 12, 16, 20, 24, 32, 48, 64$. The point where $U_{L'_B}/U_{L_B} = 1$ was taken as the transition point. This extraction finally gave the result

$$K_I = 4.95 \pm 0.05. \tag{20}$$

By flipping the sign of the fourfold field, we also confirmed numerically that the Ising transition boundaries are symmetrical with respect to the line $h_4 = 0$ [cf. Fig. 2(b)]. It is also possible to use a different order parameter ($\langle \cos \phi_i \sin \phi_i \rangle$) by rotating the spins into the first quadrant. The results using this order parameter agreed with the choice of $\langle \sin \phi_i \rangle$. We also used the order parameter blocks to estimate the critical exponent ν for the transition point, and obtained $\nu = 1.1 \pm 0.1$ in very satisfactory agreement with the exact Ising result of $\nu = 1$.

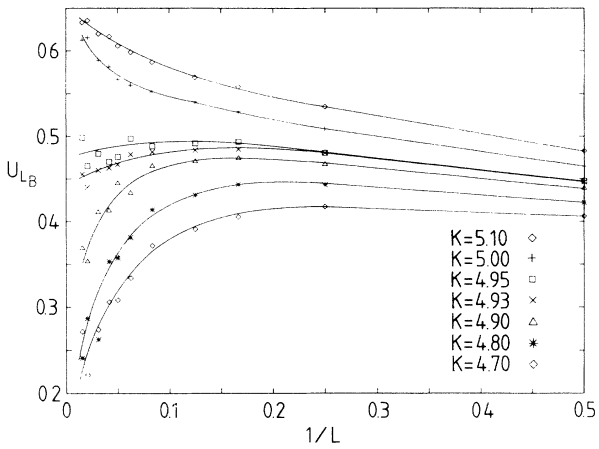

FIG. 4. Typical MCRG flows of the fourth-order cumulant vs $1/L$ for the competing case, with $h_4 = 0.06$ and $h_8 = 0.15$. When K is varied, the Ising transition occurs at around $K_I \approx 4.9$–5.0 [cf. Fig. 2(b)]. See text for details.

V. MONTE CARLO TRANSFER MATRIX METHOD

Besides Monte Carlo simulations, another numerical approach which has been quite successful in the study of statistical mechanical models is the transfer-matrix method.[15] In this method, the free energy of the model defined on an infinite strip can be obtained directly from the largest eigenvalue λ_0 of the transfer matrix as $-\ln \lambda_0$. These calculations can be done exactly for models with discrete degrees of freedom when the transfer matrix is of low order. When this technique is combined with finite-size scaling, one can obtain very accurate estimates of critical exponents and other quantities. For models with higher order transfer matrix or continuous degrees of freedom, as for the case of the XY model with symmetry-breaking fields, one has to resort to a Monte Carlo transfer-matrix (MCTM) technique[16] in order to estimate the largest eigenvalue of the transfer matrix. Some models with continuous symmetry have already been studied by this method, including frustrated XY (Refs. 17, 18) and coupled XY-Ising models.[19]

We proceed to summarize the method. Further details can be found in Refs. 15, 16, 18, and 20. The MCTM consists in a stochastic implementation of the well-known power method to obtain the dominant eigenvalue of a matrix. First, helical boundary conditions are implemeted in order to get a sparse transfer matrix. At each step a new configuration is obtained from the previous one, by adding a new spin s'_{L+1} and relabeling the sites. The infinite strip can be constructed by repetition of this identical elementary step. This process defines the transfer matrix to add a single site $T(s', s)$, where $s = s_1, s_2, \ldots, s_L$ represent a configuration of a column, with L spins. Then a sequency of random walkers $R_i = s_{1,i}, s_{2,i}, \ldots, s_{L,i}$, $1 \le i \le r$, representing the configurations of a column, is introduced with corresponding weights w_i. The number of walkers r is maintained within a few percent of a target value r_0 by adjusting

the weights properly. A matrix multiplication can be regarded as a transition process from s to s' with a probability density $P(s',s)$ defined from the elements of the transfer matrix as $T(s',s) = D(s)P(s',s)$ with a normalization factor $D(s)$ independent of s'. In each step the weights are changed according to $w_i' = D(s)w_i/c$, where $c = \lambda_0 r/r_0$ is chosen to maintain r close to r_0, with λ_0 a running estimate of the eigenvalue. In this procedure a MC step consists of a complete sweep over all random walkers. After disregarding t_0 MC steps for equilibration, an estimate of the largest eigenvalue can be obtained as

$$\lambda_0 = \frac{\sum_{t=t_0+1}^{T} c_{t+1} W_{t+1}}{\sum_{t=t_0+1}^{T} W_t}, \tag{21}$$

where $W_t = \sum_i w_{i,t}$, with $w_{i,t}$ denoting the configuration weights of a column at time t, and T is the total number of MC steps.

For the calculations of the free energy of our model we performed extensive runs using typically $r_0 = 20\,000$ random walkers and $T = 100\,000$ MC steps which corresponds to 2×10^9 attempts per spin. We concentrated our attention on two quantities, the interfacial free energy and the central charge. The former can be obtained from the free energy per site $f = -\ln \lambda_0$, as calculated from the transfer matrix on an infinite strip of width L, by a suitable choice of the boundary conditions. If antiperiodic boundary conditions are used instead of periodic ones, an interface is favored along the infinite strip and the associated interfacial free energy $\Delta F(L)$ can be obtained from the free energy difference between periodic and antiperiodic boundary conditions as

$$\Delta F(L) = L^2 \Delta f. \tag{22}$$

The finite-size scaling behavior of this quantity should drastically change as a function of temperature, depending on the relevance of the symmetry-breaking fields. At low enough temperatures this interface corresponds to a sharp boundary between two different phases due to the presence of the symmetry-breaking fields which are relevant at these temperatures, and should therefore increase as L^{d-1}. On the other hand, at higher temperatures when the symmetry-breaking field is irrelevant, the interface corresponds to a gradual change, in form of a twist of the angle ϕ, and $\Delta F(L)$ scales as L^{d-2}, which is roughly a constant at $d = 2$. In fact, in this regime ΔF ($\approx$ const) can be related to the helicity modulus (divided by $k_B T$) γ as

$$\gamma = 2\Delta F/\pi^2, \tag{23}$$

for large enough L. The change in behavior of the interfacial free energy between these regimes can be used to find the multicritical point.

Another important quantity which can be inferred from the MCTM calculations is the central charge c, which classifies the possible conformally invariant critical theories.[21] For example, $c = 1/2$ for the Ising model and $c = 1$ along the critical line of the XY model. This quantity can be related to the amplitude of the singular part of the free energy per site (at criticality) of the infinite strip by

$$f(K_c, L) = f_0 + \frac{\pi c}{6L^2} \tag{24}$$

for sufficiently large L, where f_0 denotes the regular contribution to the free energy. Although c is only defined at criticality, the value of c extracted from an $f(K,L) \times 1/L^2$ fitting of the free energy as a function of system size can be used to define an effective size- and coupling-dependent central charge $c(K,L)$ away from the critical point. According to the Zamolodchikov c theorem,[22] this quantity should have a well defined behavior near the critical point and reach a constant value, equal to the central charge, at the fixed point. As a consequence $c(K,L)$ should have a maximum near an unstable fixed point and converge to $c = 0$ in the completely disordered or ordered phases. This property is particularly useful in locating the multicritical point and the Ising transition.

To facilitate direct comparison with the MC results of Sec. III, we set $h_4 = 0$ and $h_8 = -0.15$. The results of the MCTM calculations for the central charge in this noncompeting case [cf. Fig. 2(a)] are shown in Fig. 5. The value of c was estimated by fitting the free energy per site to Eq. (24), using sizes $L = 5$ to -11. First, the abrupt onset of c near $K \approx 1$ agrees well with the known result for the XY transition (where h_8 is irrelevant). The multicritical point, on the other hand is estimated to be at the point where the central charge begins to decrease from the value of 1 (the XY phase value) to zero at $K_m = 2.6 \pm 0.4$. This is in fair agreement with the result of Eq. (16) as obtained from the histogram method; the discrepancy can be attributed to severe finite-size effects for the relatively small strip widths studied.

In Fig. 6, we show the results for the interfacial free

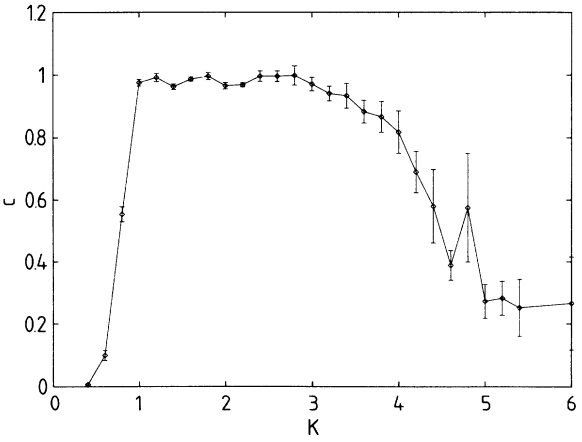

FIG. 5. MCTM results for the effective central charge along the line $h_4 = 0$, with $h_8 = -0.15$ [the noncompeting case of Fig. 2(a)]. The first abrupt onset to $c = 1$ corresponds to the KT transition, and the onset of decline of c at $K_m \approx 2.6$ indicates entry to the line of first-order phase transitions just below K_m^{-1} in Fig. 2(a).

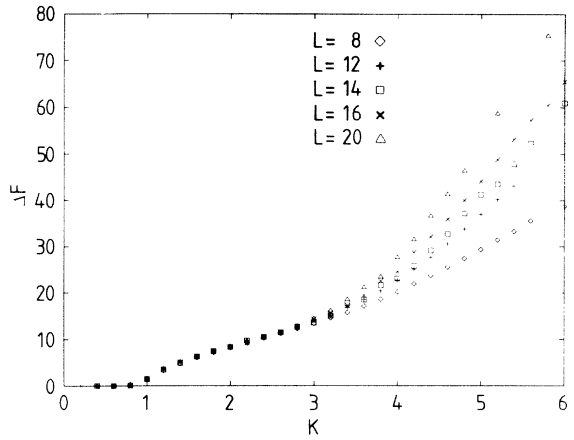

FIG. 6. The interfacial free energy from the MCTM method for different strip sizes as a function of K, for the case $h_4 = 0$ and $h_8 = -0.15$ as in Fig. 5. Below $K_m \approx 2.6$, the lack of size dependence of the energy indicates the onset of the spin wave regime corresponding to a line of XY transitions. The corresponding value of K^* is in good agreement with the theoretical prediction $8/\pi$. See text for details.

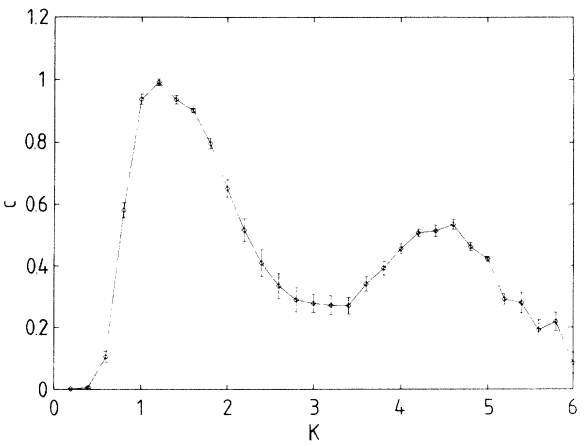

FIG. 7. MCTM results for the effective central charge with $h_4 = 0.06$, $h_8 = 0.15$, corresponding to the competing case of Fig. 2(b). The first peak at $c = 1$ corresponds to the KT transition point, while the second peak at $K_I \approx 4.6$ verifies the expected Ising transition, with $c = 1/2$.

energy for different strip widths L as a function of temperature for the same noncompeting case. One clearly sees a size dependence at large values of K indicating the relevance of the symmetry-breaking field h_8. At temperatures above $K_m^{-1} \approx 1/2.6$ the size dependence is practically absent, indicating the spin wave regime of the critical line of the XY model. In this regime the helicity modulus is equal to the renormalized coupling constant K^* and should be equal to $K^* = 8/\pi$ at K_m. As indicated in Fig. 6, the helicity modulus $\gamma = 2\Delta F/\pi^2$ is in good agreement with the expected result. Moreover, the termination point of the lines at $\Delta F = 0$ is in good agreement with the KT transition point.

Next, we use the MCTM method to study the Ising transition in the case of competing h_4 and h_8 fields. As in Sec. IV, we set $h_4 = 0.06$ and $h_8 = 0.15$. The results for c vs K are shown in Fig. 7. The effective central charge has two peaks as a function of temperature. At high temperatures the peak value is very close to $c = 1$, which is consistent with a transition in the universality class of the XY model with a fourfold field. The other peak at low temperatures is close to $c = 1/2$ which is consistent with an Ising transition. The Ising transition can be estimated simply from the peak value of c yielding $K_I = 4.6 \pm 0.4$. These results are again in reasonable agreement with the MCRG method, Eq. (20).

VI. SUMMARY AND DISCUSSION

In this work, we have analyzed in detail the properties of the two-dimensional XY model in the presence of fourfold and eightfold symmetry-breaking fields h_4 and h_8, respectively. First we have applied mean-field and renormalization-group arguments to predict that, when the h_4 field changes from positive to negative values, there is a phase transition between a phase with the order parameter pointing along the $\phi = \pi/4$ direction, and another phase with the corresponding order parameter pointing along the $\phi = 0$ direction. This phase transition is continuous at high temperatures where the eightfold field is irrelevant. In this case, right at the phase boundary all the symmetry-breaking fields are absent and the system is in the ordered phase of a pure XY model with only algebraic long-range order. At lower temperatures when the eightfold field is relevant, the nature of the transition now depends crucially on whether h_8 and h_4 are compatible or competing with each other. In the former case, the transition becomes first order and there is a multicritical temperature separating the high temperature and low temperature phase boundary. In the competing case the first-order phase transition splits into two transitions, both of which are in the Ising universality class. The order parameter rotates continuously from the $\phi = 0$ direction towards the $\phi = \pi/4$ direction in between the two Ising phase boundaries. We note that similar effects can result from the competition of sixfold and twelvefold fields as discussed by Selinger and Nelson[5] in their study of liquid crystals.

We have then performed a detailed numerical analysis of our model Hamiltonian through Monte Carlo simulations. Because of the large finite-size effects, the finite-size simulation data have to be extrapolated to infinite size through finite-size scaling concepts and numerical renormalization-group analysis. We have first confirmed the qualitative nature of the phase boundary as discussed above. We have then employed the recently developed histogram techniques to locate the multicritical temperature. Finally, in the case of the competing fields, we have used Binder's block renomalization technique to identify the Ising-like transitions. These results have further been corroborated by Monte Carlo transfer-matrix techniques. All our numerical results are in good agreement with theoretical arguments.

Our model was originally motivated by the study of the H/W(100) chemisorption system. We have shown

previously that the critical properties of this system in the ordered $c(2 \times 2)$ phase can be described by an XY model with four- and eightfold symmetry-breaking fields. The effect of the adsorbed hydrogen in the low coverage limit is to change the effective fourfold field. Thus increasing the hydrogen coverage in this system is tantamount to changing the fourfold field from negative to positive values in the model Hamiltonian studied in this paper. In addition, our previous work showed[6] that the adsorbed hydrogen also generates an eightfold field which is compatible with the fourfold field. Experimental evidence from an infrared spectroscopy study[23] for this system supports the scenario of a continuous transition from $\langle 11 \rangle$ (corresponding to negative h_4) to $\langle 10 \rangle$ (positive h_4) phase at room temperature when the hydrogen coverage is increased. On the other hand, the low energy electron diffraction study of Griffiths *et al.*[24] showed indications of coexistence between the two phases for coverages in the range from about 0.05 to 0.16 ML, which indicates a first-order transition. This is exactly the behavior of our model Hamiltonian studied in this paper when the fields h_4 and h_8 are compatible. Thus the qualitative agreement between the experimental data and the theory presented here is gratifying. In view of the very rich behavior of the phase diagram, especially near the multicritical point, more experimental studies of the switching transition in this system and comparison with the theoretical predictions here would be most fruitful.

ACKNOWLEDGMENTS

This work has been supported by the Conselho Nacional de Desenvolvimento Científico e Tecnológico (CNPq)–NSF International Collaboration program. T.A-N. and K.K. have been partly supported by the Academy of Finland, S.C.Y. by an ONR grant, and J.M.K. by an NSF grant. E.G. acknowledges the support from Fundação de Amparo à Pesquisa do Estado de São Paulo (FAPESP, No. 92/0963-5) and CNPq. The Center for Scientific Computing and Tampere University of Technology are acknowledged for the computational resources.

[1] J. M. Kosterlitz and D. J. Thouless, J. Phys. C **6**, 1181 (1973); J. M. Kosterlitz, *ibid.* **7**, 1046 (1974).
[2] N. D. Mermin and H. Wagner, Phys. Rev. Lett. **17**, 1133 (1966).
[3] N. D. Mermin, Phys. Rev. **176**, 250 (1968).
[4] J. V. José, L. P. Kadanoff, S. Kirkpatrick, and D. R. Nelson, Phys. Rev. B **16**, 1217 (1977).
[5] J. V. Selinger and D. R. Nelson, Phys. Rev. Lett. **61**, 416 (1988); Phys. Rev. A **39**, 3135 (1989).
[6] K. Kankaala, T. Ala-Nissila, and S.-C. Ying, Phys. Rev. B **47**, 2333 (1993).
[7] D. D. Betts, Can. J. Phys. **42**, 1564 (1964).
[8] U. Wolff, Phys. Rev. Lett. **62**, 361 (1989).
[9] C. F. Baillie and P. D. Coddington, Concurrency **3**, 129 (1991).
[10] K. Kankaala (unpublished); T. Rautiainen and K. Kankaala (unpublished).
[11] R. Ben-Avi and G. Bhanot (unpublished).
[12] J. Lee and J. M. Kosterlitz, Phys. Rev. Lett. **65**, 137 (1990); Phys. Rev. B **43**, 1268 (1991); **43**, 3265 (1991).
[13] A. M. Ferrenberg and R. H. Swendsen, Phys. Rev. Lett. **61**, 2635 (1988).
[14] K. Binder, Phys. Rev. Lett. **47**, 693 (1981); Z. Phys. B **43**, 119 (1981).
[15] M. P. Nightingale, in *Finite Size Scaling and Numerical Simulations of Statistical Systems*, edited by V. Privman (World Scientific, Singapore, 1990).
[16] M. P. Nightingale and H. W. J. Blöte, Phys. Rev. Lett. **60**, 1562 (1988).
[17] E. Granato, Phys. Rev. B **45**, 2557 (1992); **48**, 7727 (1993).
[18] E. Granato and M. P. Nightingale, Phys. Rev. B **48**, 7438 (1993).
[19] E. Granato, J. M. Kosterlitz, J. Lee, and M. P. Nightingale, Phys. Rev. Lett. **66**, 1090 (1991); M. P. Nightingale, E. Granato, and J. M. Kosterlitz (unpublished).
[20] M. P. Nightingale, in *Proceedings of the Third International Conference on Supercomputing*, edited by L. P. Kartashev and S. I. Kartashev (International Supercomputing Institute, Inc., Boston, 1988), Vol. I, p. 427.
[21] H. W. Blöte, J. L. Cardy, and M. P. Nightingale, Phys. Rev. Lett. **56**, 742 (1986).
[22] A. B. Zamolodchikov, Pis'ma Zh. Eksp. Teor. Fiz. **43**, 567 (1986) [JETP Lett. **43**, 733 (1986)].
[23] J. J. Arrecis, Y. J. Chabal, and S. B. Christman, Phys. Rev. B **33**, 7906 (1986).
[24] K. Griffiths, D. A. King, and G. Thomas, Vacuum **31**, 671 (1981).